Research Article

Efficiency of Ferritin as an MRI Reporter Gene in NPC Cells Is Enhanced by Iron Supplementation

Yupeng Feng,[1, 2] Qicai Liu,[3] Junfeng Zhu,[4] Fukang Xie,[5] and Li Li[1]

[1] *State Key Laboratory of Oncology in Southern China, Imaging Diagnosis and Interventional Center, Cancer Center, Sun Yat-sen University, 651 Dongfeng Road East, Guangzhou 510060, China*
[2] *Department of Urinary Surgery, Affiliated Xixiang People's Hospital of Guangdong Medical College, Shenzhen 518102, China*
[3] *Experimental Medical Research Center, Guangzhou Medical College, 195 Dongfeng Road West, Guangzhou 510182, China*
[4] *Department of Pathology, The First Affiliated Hospital of Sun Yat-sen University, Guangzhou 510080, China*
[5] *Department of Anatomy and Histoembrology, Zhongshan School of Medicine, Sun Yat-sen University, Guangzhou 510080, China*

Correspondence should be addressed to Li Li, li2@mail.sysu.edu.cn

Background. An emerging MRI reporter, ferritin heavy chain (FTH1), is recently applied to enhance the contrast and increase the sensitivity of MRI in the monitoring of solid tumors. However, FTH1-overexpression-related cytotoxicity is required to be explored. *Methods*. By using the Tet-Off system, FTH1 overexpression was semi-quantitatively and dynamicly regulated by doxycycline in a NPC cell line. Effects of FTH1 overexpression on the proliferation, cytotoxicity, apoptosis and migration of NPC cells were investigated *in vitro*, and MR relaxation rate was measured *in vitro* and *in vivo*. *Results*. *In vitro* and *in vivo* overexpression of FTH1 significantly increased the transverse relaxivity (R_2), which could be enhanced by iron supplementation. *In vitro*, overexpression of FTH1 reduced cell growth and migration, which were not reduced by iron supplementation. Furthermore, cells were subcutaneously inoculated into the nude mice. Results showed FTH1 overexpression decreased tumor growth in the absence of iron supplementation but not in the presence of iron supplementation. *Conclusion*. To maximize R_2 and minimize the potential adverse effects, supplementation of iron at appropriate dose is recommended during the application of FTH1 as a reporter gene in the monitoring of NPC by MRI.

1. Background

Magnetic resonance imaging (MRI) is widely used in the diagnosis, staging, followup, and prediction of diseases in clinical practice [1–4]. In the biological research, MRI has been applied to monitor the growth of solid tumors, gene expression, angiogenesis, and apoptosis in various animal models [5–8]. MRI allows views into opaque subjects and provides soft-tissue contrast at reasonably high spatial resolution. However, the low sensitivity and specificity of MRI significantly limited its wide application.

It has been reported that ferritin gene, an emerging MRI reporter gene, can enhance the contrast and increase the sensitivity of MRI [9–11]. In vertebrates, ferritin is a heteropolymer composed of variable proportions of heavy and light chains. Twenty-four heavy and light chains assemble to form a ferritin molecule. The ferritin heavy chain (FTH1) is the major regulator of ferritin activity. FTH1 has ferroxidase activity promoting the iron oxidation and incorporation. In contrast, the light chain lacks the detectable ferroxidase activity but increases the activity of FTH1 [12]. Unlike superparamagnetic iron oxide particles (SPIOs) and other particle-based techniques [13, 14], the genetic modified transgene of FTH1, like other MR reporters, [15, 16] would not be diluted when cells divide. In this regard, the continuous production of FTH1 in the daughter cells offers a significant advantage for cell tracking by MRI over a particle-based cell labeling method. So far, a few studies have focused on FTH1 as an emerging reporter, in which overexpression of FTH1 can alter the MR signal in its expression site and

yield robust image contrast [9, 10, 15–21]. However, no studies have tested the role of FTH1 in the nasopharyngeal carcinoma (NPC) cells.

The results on the FTH1 as a safe MRI reporter were inconsistent in previous studies. Cozzi et al. [22] demonstrated that overexpression of FTH1 in the Hela cells induced an iron-deficient phenotype with significantly reduced cell growth, which could be reversed by incubation in the iron-containing medium. Overexpression of FTH1 in the C6 glioma cells [9] and stem cells [17] did not reduce cell growth even in the absence of iron supplementation. However, Liu et al. [16] described in the discussion section (data not shown) of their paper that significant reduction of growth rate was observed in the C6 glioma cells in the presence of high FTH1 transgene expression. Based on these findings, the present study aimed to investigate the potential adverse effects of FTH1 on NPC cells.

NPC is a nonlymphomatous squamous cell carcinoma arising from the mucosal epithelium of the nasopharynx. NPC is common in southern regions of China, Northern Africa, and Alaska [23]. The poor survival rate and high recurrence prompt us to find new therapeutic approaches for this disease. However, the development of treatment for NPC has been hampered due to lack of conventional cells and animal models for the effective, noninvasive, spatiotemporal, and real-time monitoring of therapeutic efficacy. In the present study, the NPC cell model was employed.

In our study, FTH1 overexpression was semiquantitatively controlled by using doxycycline in the Tet-Off system aiming to investigate the therapeutic effect of FTH1 and further assess the potential adverse effects of FTH1 as an MRI reporter in NPC cells.

2. Methods

2.1. Construction of Plasmids and Reverse Transcription PCR (RT-PCR).
The open reading frame (ORF) of human FTH1 gene with Kozak sequence was amplified by RT-PCR from the total RNA of S18 cells and then subcloned into the SmaI site of pUC119 to yield pUC119-FTH1. After sequencing, the fragment released by BglII and EcoRI from pUC119-FTH1 was cloned into the same site of pTRE-Tight-BI-Luc (Clontech Laboratories, Inc., Palo Alto, CA) to yield pTRE-Tight-BI-Luc-FTH1. For RT-PCR, the first strand cDNA was reversely transcribed with oligo (dT) primer. The full-length FTH1 gene with Kozak sequence was amplified using PrimeSTAR HS DNA Polymerase (TaKaRa, Dalian, China). The sense primer was 5′-GAATTCGCCACCATG-ACGACCGCGTCCACCTC-3′ and the antisense primer 5′-AGATCTGGTACCTTTAGCTTTCATTATCACTGTC-3′.

2.2. Cell Culture.
NPC S18 cells (kindly gifted by Dr. Chaonan Qian) [24] were grown in Dulbecco's Modified Eagle's Medium (DMEM)—high glucose (GIBCO, Grand Island, N.Y.) containing 10% fetal bovine serum (FBS; Clontech Laboratories, Inc., Palo Alto, CA). The parent cells, which were developed by stably transfecting pTet-Off Advanced vector into S18 cells, were grown in complete DMEM containing 100 μg/mL G418 (Clontech Laboratories, Inc., Palo Alto, CA). The double-stable cell line (B-7) was grown in complete DMEM containing 100 μg/mL G418 and 100 μg/mL hygromycin (Alexis Biochemicals, San Diego, CA) with or without 10 ng/mL doxycycline (Alexis Biochemicals, San Diego, CA). In the experiments with iron supplementation, ferric ammonium citrate at different concentrations (FAC; Sigma-Aldrich Biotechnology, St. Louis, MO) was added to the medium.

2.3. Transfection Protocol and Generation of Stable Cell Clones.
Cells were transfected using Lipofectamine2000 (Invitrogen, Carlsbad, CA) according to the manufacturer's instructions. The NPC S18 cells were first transfected with pTet-Off Advanced vector and screened in complete medium containing 500 μg/mL G418. The screened clones (parent cell) were then transfected with pTRE-Tight-BI-Luc-FTH1. These cells were screened in the presence of 500 μg/mL G418, 250 μg/mL hygromycin, and 10 ng/mL doxycycline. The well-grown clones were subjected to screening of expression of luciferase and FTH1. Several double-stable clones were selected and the B-7 clone was used in the following experiments.

2.4. Detection of Luciferase Activity.
Cells (1×10^4/well) were plated into 96-well plates, grown for 48 h, and washed twice with phosphate-buffered saline (PBS). The cells were lysed, and then assayed for the luciferase activity with the luciferase assay system, in accordance with the manufacturer's instructions (Promega, Madisson, WI, USA). The luciferase activity was measured with the GloMax 96 Microplate Luminometer (Promega, Madisson, WI, USA) using standard protocol. The luminescence results were reported as arbitrary light units that were measured in 10 seconds per sample. To measure the luciferase activity *in vivo*, mice were anesthetized and D-luciferin solution (Promega, Madisson, WI, USA) was intraperitoneally injected at 125 mg/kg body weight 10 min prior to imaging. A gray-scale body-surface reference image was obtained using the NightOWL LB 981 NC 100 CCD camera (Berthold, Wildbad, Germany). Photons emitted from the luciferase of animals and transmitted through the tissues were collected and integrated for a 5-minute period. The signal intensities from manually derived regions of interest (ROI) were obtained and data expressed as photon flux (photons/sec). Background photon flux was defined from an ROI of same size being placed in a nonluminescent area nearby the animal and then subtracted from the measured luminescent signal intensity (SI).

2.5. Western Blot and Immunohistochemistry.
Cells were lysed in RIPA buffer. Total protein concentration was determined by bicinchoninic acid (BCA) method. Then, 25 μg of total proteins were subjected to 12% SDS-PAGE and transferred onto polyvinylidene fluoride (PVDF) membranes which were then blocked in 5% nonfat milk in TBST (20 mM Tris PH 7.6, 137 mM NaCL, 0.1% Tween20). Subsequently, these membranes were incubated with primary antibodies overnight at 4°C (rabbit anti-FTH1 1 : 1000 (Santa Cruz Biotechnology, California, USA), rabbit anti-GAPDH

1 : 2000 (GenScript, Nanjing, China)). After washing several times, the membranes were treated with secondary antibodies (HRP-conjugated goat anti-rabbit 1 : 5,000 (Invitrogen, Carlsbad, CA)), and visualized using the enhanced chemiluminescence kit.

FTH1 expression in the xenografted tumors was detected by immunohistochemistry. At the end of 3 weeks, mice were sacrificed and the xenografted tumors were cut into 4 μm sections. Following treatment with anti-FTH1 antibody, these sections were treated with biotinylated anti-rabbit secondary antibody and then ABC reagent (Invitrogen, Carlsbad, CA), and visualized using diaminobenzidine (DAB).

2.6. Determination of Iron Content. Inductively coupled plasma mass spectrometry (ICP-MS) was employed to qualitatively determine the iron content in cells and tumors (cells: 10^6 cells/sample; tumors: Fe content normalized by the dry weight).

2.7. Detection of Cell Proliferation, Cytotoxicity, and Apoptosis. The cell proliferation kit I (MTT-based) was used to detect the cell proliferation according to the manufacturer's instructions (Roche Diagnostics, Mannheim, Germany). Cytotoxicity was measured by detecting the amount of enzyme glucose-6-phosphate dehydrogenase (G6PD) released into the medium according to the manufacturer's instructions (Invitrogen, Carlsbad, CA). For apoptosis assay, Hoescht staining was used according to vendor protocol (Promega, Madisson, WI, USA).

2.8. Migration Assay. Migration assay was performed using the 24-well transwell inserted with a polycarbonate membrane (6.5 mm in diameter, 8.0 μm in pore size, Costar). The lower chamber was filled with standard medium. The upper chamber was seeded with 2×10^4 B-7 cells/well in conditional medium with or without 200 μM FAC. Cells were allowed to migrate for 24 h at 37°C and then stained in PBS containing 50 μg/mL propidium iodide. Cells on the upper surface of the membrane were removed with a cell scraper and migrated cells on the lower surface fixed in 4% paraformaldehyde and counted. The proportion of migrating B-7 cells in the standard medium served as a control and were defined as 100%. The proportion of migrating B-7 cells in other conditions was calculated as the percentage of control value.

2.9. MRI In Vitro. Cells were thoroughly washed to remove free iron and dissociated with trypsin, followed by fixation in 4% paraformaldehyde for 10 min. The cells in 96-well plate (5×10^7 cells/well) were centrifuged at 1000 rpm for 5 min (Beckman, CA, USA) and supernatant was removed. Then, 100 μL of 1% agarose in PBS were added to the cell pellet which remained as pellet in the agarose. Transverse relaxation rate (R_2, $R_2 = 1/T_2$) was determined from spin-echo image at GE Signa 1.5 T MR Scanner (multiecho spin echo; TR: 4000 ms; seven echo times: 40, 80, 120, 200, 240, 280 and 320 ms; matrix: 128 $\times$ 128; FOV: 40 $\times$ 40 mm). A horizontal slice was selected using orthogonal images,

through the center of cell pellet of all wells (2 mm in slice thickness). ROIs of each cell pellet were drawn manually in a slice through the center of cell pellet, and the mean SI was measured using the software for system. The natural logarithm of SI was plotted as a function of TE, and the R_2 value was calculated as the negative of the slope of a regression line fit to the data (Excel, Microsoft Inc.). These measurements were repeated in triplicates and data presented as mean $\pm$ standard deviation (SD). Data were analyzed with the two-tailed unpaired Student's t-test.

2.10. MRI In Vivo. All mice used in these experiments were maintained under the protocols approved by the Institutional Animal Care and Use Committee of Sun Yat-sen University. Cells were subcutaneously inoculated (10^6 cells/mouse) into hind flank of BALB/c-nude mice (females, 6–10 weeks, 28–30 g). At the indicated time points, MRI was performed using a Siemens 3.0 T Trio MR scanner (TE: 40 ms, TR: 6000 ms, FOV: 60 $\times$ 60 mm, matrix: 300 $\times$ 300, slice thickness: 2 mm). T_2 and R_2 were calculated by fitting decay curves delineated from a Carr-Purcell-Meiboom-Gill (CPMG) sequence. Changes in the relaxation rate were determined by selection of an ROI (for tumors or cell pellets) on the relaxation maps. Data were expressed as mean $\pm$ SD and analyzed with the two-tailed unpaired Student's t-test.

Tumor volumes were calculated based on the MR images at the end of 1, 2, and 3 weeks according to the following formula: volume = width$^2 \times$ length $\times$ 0.52 [25] in the absence of iron supplementation.

3. Results

3.1. Overexpression of FTH1 in NPC S18 Cells. Tet-Off Advanced system was used to generate a cell model with controlled gene expression [26]. NPC S18 cells were stably transfected with pTet-Off Advanced vector and the clones expressing doxycycline-dependent regulator were selected and used as parent cells. FTH1 was cloned into the pTRE-Tight-BI-Luc vector and under the control of inducible doxycycline responsive promoter (Figure 1(a)). The resulted vectors, which could simultaneously express luciferase and FTH1 under the control of same promoter, were used to transfect the parent cells. Among the stable transfectant clones, one was selected and named as B-7. B-7 cells were grown in the presence (Dox+) or absence (Dox−) of 10 ng/mL doxycycline for 48 h, to test whether luciferase activity could be induced by doxycycline. As shown in Figure 1(b), luciferase activity of B-7 cells in the absence of doxycycline was 3000-fold higher than that in the presence of doxycycline. Additionally, B-7 cells in presence of doxycycline were transferred to medium without doxycycline and grown for different durations. The time-dependent expression of FTH1 was determined by Western blot assay. Results showed the FTH1 level increased gradually within 72 h and then remained stable (Figure 1(c)). Furthermore, B-7 cells were grown in medium containing doxycycline

(a)

(b)

Dox− (hours) 0 24 48 72 96

FTH1

GAPDH

(c)

Dox+ (ng/mL) 0 0.1 10

FTH1

GAPDH

(d)
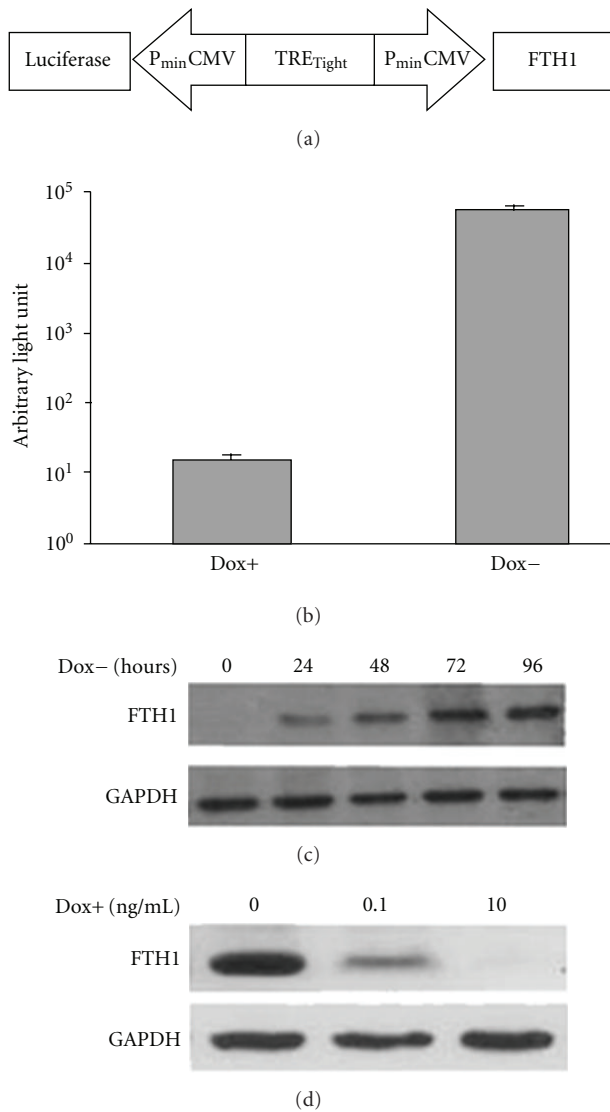
FIGURE 1: Doxycycline-regulated expression of luciferase and FTH1 in NPC S18 cells. (a) The schematic for the preparation of pTRE-Tight-BI-Luc-FTH1 used to generate the double-stable cell line, B-7, which could inducibly express luciferase and FTH1 simultaneously under the control of same promoter. (b) Luciferase activity induced by doxycycline. B-7 cells were grown in presence (Dox+) or absence (Dox−) of 10 ng/mL doxycycline for 48 h. Cells were analyzed for luciferase activity. Data were expressed as mean ± SD from 3 experiments. (c) Time-dependent FTH1 expression. B-7 cells grown in Dox containing medium were transferred to medium without Dox and grown for different durations. (d) Doxycycline dose-dependent FTH1 expression. B-7 cells were grown in medium containing doxycycline at different concentrations for 96 h. FTH1 was determined by Western blot assay. Dox, doxycycline.

at different concentrations for 96 h to determine the dose-dependent expression of FTH1. FTH1 expression was maximally inhibited when the doxycycline concentration was ≥10 ng/mL and increased to a moderate level when the doxycycline was 0.1 ng/mL. It was completely derepressed when doxycycline was absent (Figure 1(d)). In the repressed

Dox− (hours) 0 72

TfR-1

GAPDH

(a)

(b)

(c)
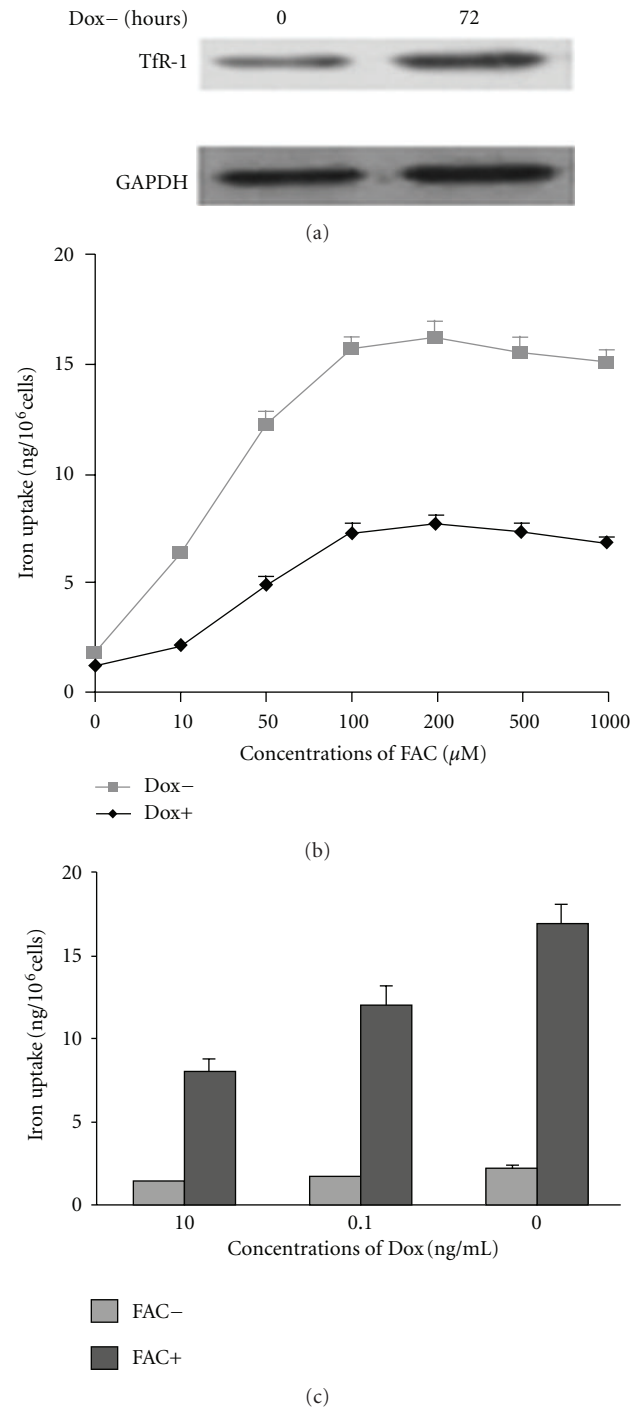
FIGURE 2: Overexpression of FTH1 led to increase of both transferrin receptor 1 (TfR-1) and intracellular iron content. (a) Western blot assay of TfR-1 expression induced by FTH1. B-7 cells grown in the presence of doxycycline (10 ng/mL) (Dox+) were transferred to Fe containing medium (200 μM FAC) in absence of doxycycline (Dox−) followed by incubation for 72 h. (b, c) Quantification of intracellular iron content by ICP-MS. (b) B-7 cells were grown in the presence (Dox+) or absence (Dox−) of doxycycline (10 ng/mL) in the presence of FAC at different concentrations for 48 h, (c) B-7 cells grown in the presence of doxycycline at various concentrations were incubated with (FAC+) or without (FAC−) (200 μM) for 48 h. Data were expressed as mean ± SD from 3 experiments. FAC, ferric ammonium citrate. ICP-MS, inductively coupled plasma atomic emission spectrometry.
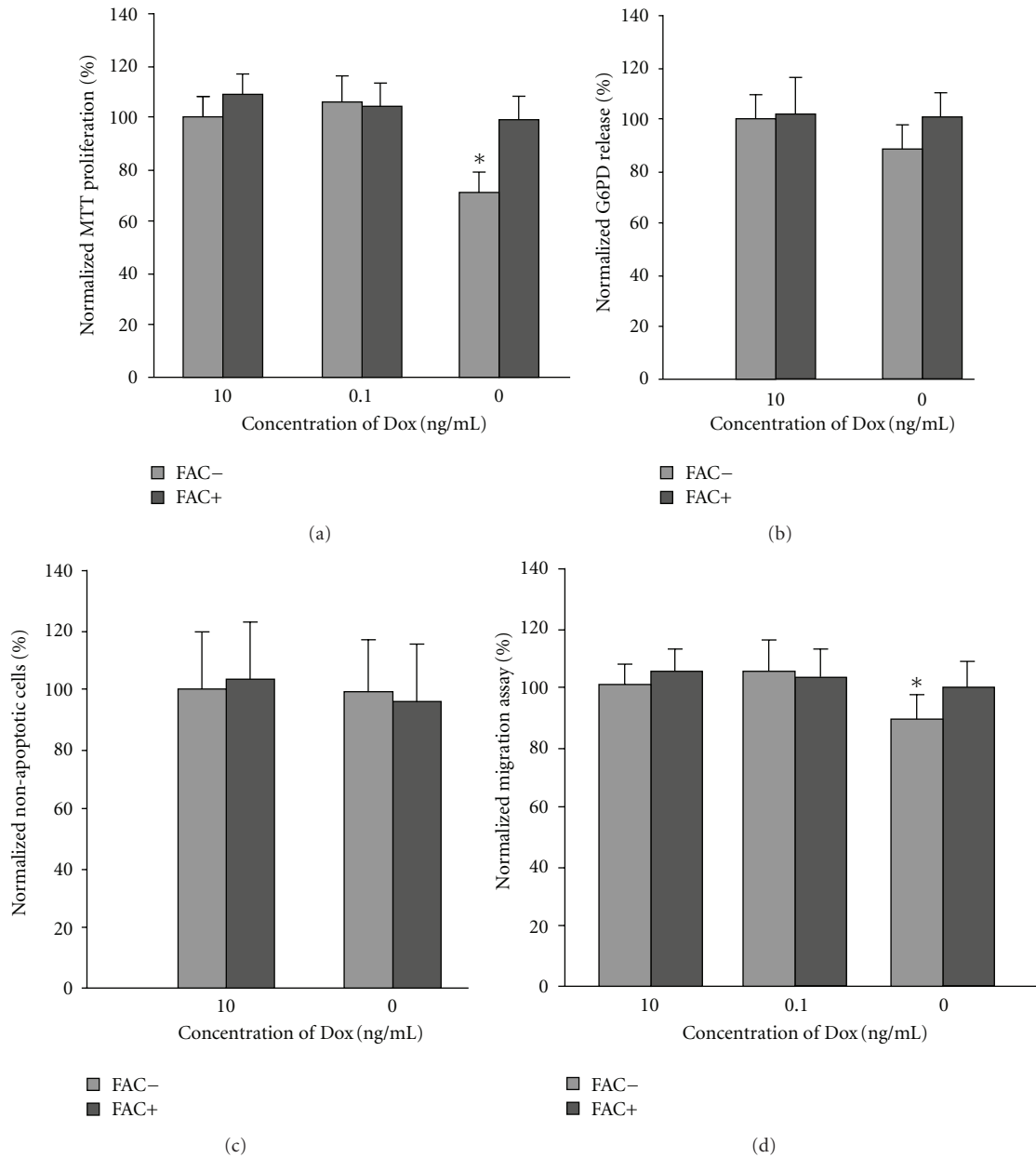
(a)

(b)

(c)

(d)

FIGURE 3: Effects of FTH1 overexpression on cell proliferation, cytotoxicity, apoptosis, and migration. (a) High expression of FTH1 reduced cell growth without iron supplementation while did not reduce cell growth with iron supplementation. MTT assay was used to assess the effect of FTH1 overexpression on the cell proliferation. (b) FTH1 overexpression did not increase the release of G6PD regardless of Fe supplementation. High G6PD release represents increased toxicity. (c) FTH1 overexpression did not increase the cell apoptosis by hoechst apoptosis assay regardless of iron supplementation. (d) High expression of FTH1 reduced cell migration without iron supplementation while did not reduce cell migration with iron supplementation. Data were normalized by those in B-7 cells in 10 ng/mL Dox which was defined as 100%; G6PD, glucose-6-phosphate dehydrogenase. Data were expressed as mean ± SD from 6 experiments. ($^*P < 0.05$: two-tailed unpaired t-test.)

state, slightly higher FTH1 level than that in the parent cells might be due to the leakiness.

FTH1 and transferrin receptor-1 (TfR-1) production are tightly regulated by the labile iron pool (LIP) level [27]. Thus, FTH1 overexpression may increase the Fe storage and reduce the LIP, which in turn leads to an upregulation of TfR-1. To test whether FTH1 can induce this effect in NPC S18 cells,

the TfR-1 levels were measured in the repressed and de-repressed state using Western blot assay (Figure 2(a)). A statistically significant increase, ~56%, in the TfR-1 level was observed in the de-repressed state as compared to that in the repressed state.

FTH1 overexpression may trigger an increase in the cell's ability to internalize and store Fe. The relevance of
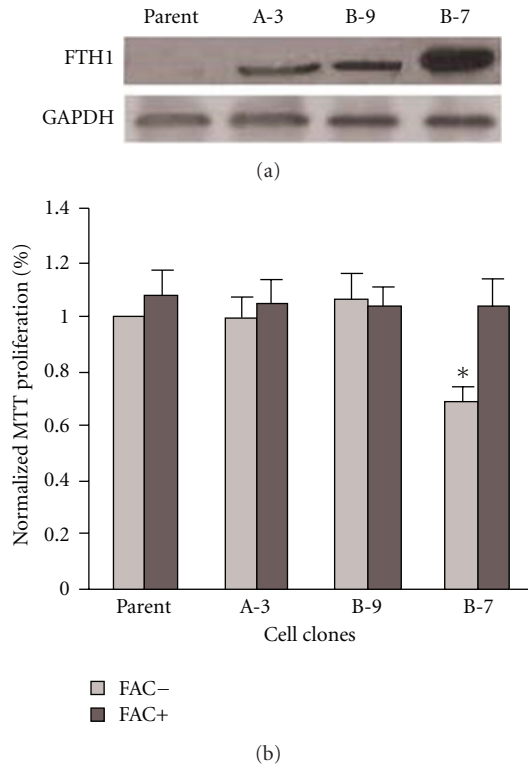
(a)

(b)

FIGURE 4: Effects of FTH1 overexpression on cell proliferation in other two clones. (a) FTH1 expression in different cell clones was measured by western blot assay. (b) Effect of FTH1 overexpression on cell proliferation. MTT assay was used to assess the effect of FTH1 overexpression on cell proliferation. Data were normalized by those in parent cells without FAC supplementation. Data were expressed as mean ± SD from 3 experiments. Parent cells grown in absence of FAC were set as control. ($*P < 0.001$.)

intracellular iron content with the overexpression of FTH1 in response to FAC at different concentrations was confirmed by ICP-MS analysis. As shown in Figure 2(b), FAC caused a dose-dependent increase of intracellular iron content. The maximal intracellular iron content was achieved at 100∼200 μM FAC and further increase of FAC concentration did not raise the intracellular iron content. At the same concentration of FAC (200 μM), the intracellular iron content was affected by the FTH1 expression. When the doxycycline concentration decreased from 10 ng/mL to 0 ng/mL, the iron uptake increased due to a high FTH1 expression. These results indicate that high FTH1 expression may increase the iron uptake when the iron is available (Figure 2(c)).

3.2. Effects of FTH1 Overexpression on Proliferation, Cytotoxicity, Apoptosis, and Migration.

B-7 clones could be maintained in the medium without doxycycline for up to two months showing no evident toxicity. However, the clones reached confluence more rapidly in the presence of doxycycline (10 ng/mL) than that in absence, whereas doxycycline at 10 ng/mL had no evident effects on B-7 cell growth.

To assess whether FTH1 transgene expression is detrimental to cell viability, methyl thiazole tetrazolium (MTT)

assay was used to measure the cellular proliferation (Figure 3(a)). When cells were grown at 0.1 ng/mL doxycycline, moderate overexpression of FTH1 did not affect cell growth with or without Fe supplementation. While cells were grown in absence of doxycycline, high expression of FTH1 had different effects: the cell growth rate was decreased by 30% without Fe supplementation, but the growth rate remained unchanged in the presence of Fe supplementation when compared with that at the repressed state (10 ng/mL doxycycline). In other clones, cell growth at relatively high level of FTH1 was independent of iron supplementation (Figure 4). Ferritin level in these clones was much lower relative to B-7 clone, and therefore, it is possible that expression level was not high enough to affect cell growth.

To further address the potential cytotoxicity of overexpression of FTH1, we detected the G6PD released into the medium. No difference in the G6PD was found between FTH1 overexpressed cells and FTH1-depressed cells regardless of iron supplementation (Figure 3(b)).

In addition, the effect of FTH1 overexpression on the apoptosis was also studied. Results showed no significant increase in the apoptosis of FTH1 over-expressed cells as compared to FTH1 depressed cells regardless of iron supplementation (Figure 3(c)).

The tumor metastasis has great impact on the recurrence and prognosis of cancer in clinical practice. The NPC S18 cells are easy to migrate *in vitro* [24]. Whether FTH1 overexpression has influence on the tumor migration is important for FTH1 as an MRI reporter. Thus, the effect of FTH1 overexpression on the migration of S18 cells *in vitro* was measured. As shown in Figure 3(d), overexpression of FTH1 reduced the cell migration, which was reverse following Fe supplementation.

3.3. Changes in Magnetic Relaxation Properties of B-7 Cells In Vitro.

T_2-weighted images and transverse relaxation rates (R_2) of B-7 cells under different conditions are shown in Figure 5. Results demonstrated a significant increase of R_2 upon induction of FTH1 overexpression and iron supplementation. Fe supplementation significantly increased the R_2, which reached the maximal level at 200 μM FAC but further increase of FAC concentration did not additionally increase the R_2. At 0.1 ng/mL doxycycline, the R_2 was lower than that in the absence of doxycycline, but higher than that in presence of 10 ng/mL doxycycline. These results indicate both FTH1 expression and iron availability are important for the induction of R_2.

3.4. Iron Supplementation Enhanced MRI Signal and Reduced the Affection on Cell Growth of FTH1 In Vivo.

To determine the changes in R_2 relaxation rates relevant to FTH1 overexpression *in vivo*, B-7 cells and parent cells were inoculated subcutaneously to BALB/c-nude mice. These mice were administered with or without FAC in drinking water (2 g of FAC in 1 L of water) [28]. All the mice were not treated with doxycycline. As shown in Figures 6(a)–6(c), R_2 was higher in B-7-cell-induced tumors than that in parent-cell-induced tumors, and Fe supplementation
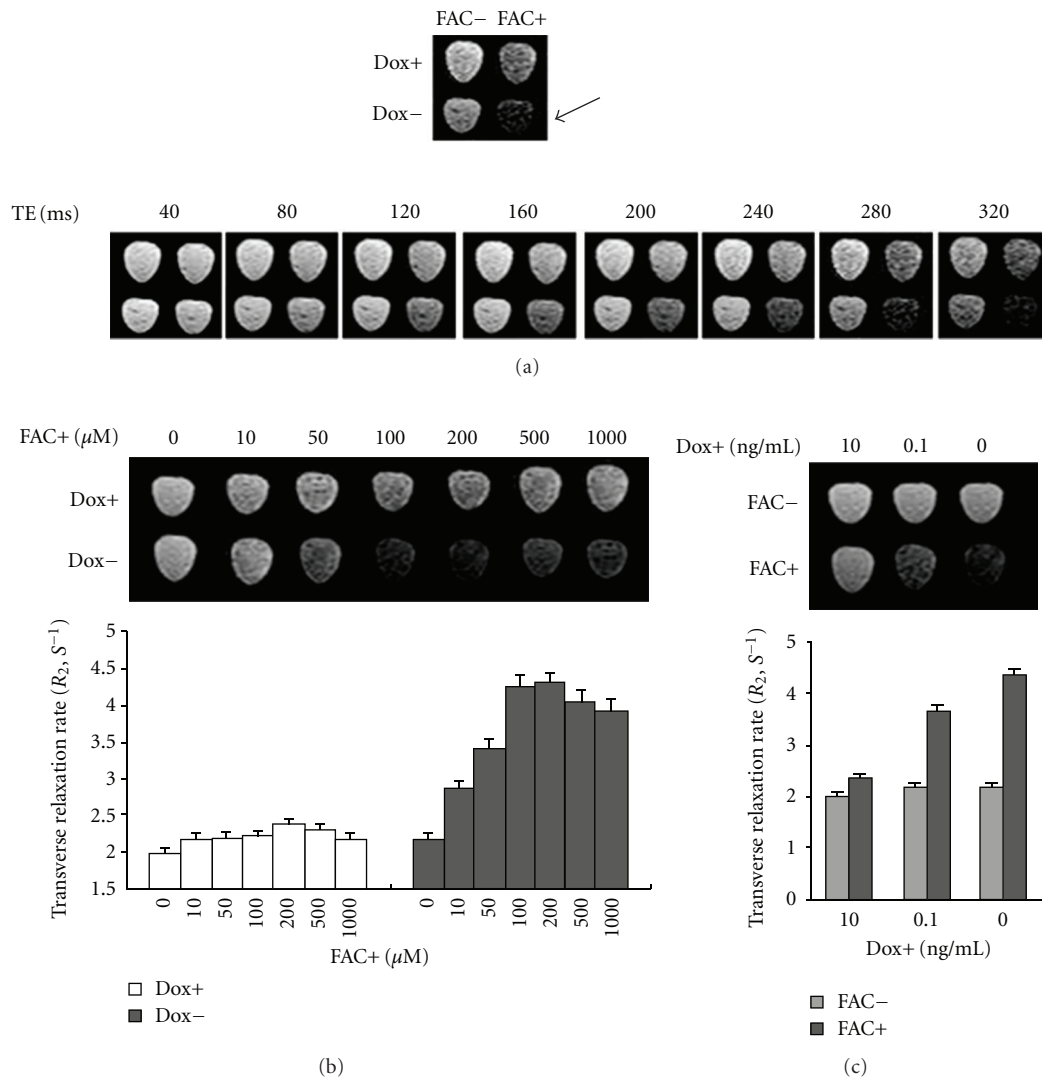
FIGURE 5: B-7 cells under both derepressed state (FTH1 overexpression) and the presence of FAC supplementation was capable of producing visible contrast by MRI. (a) B-7 cells were cultured with or without 10 ng/mL doxycycline and with or without FAC for T_2-weighted images. Arrow indicated the sample with the highest R_2, in the presence of both FTH1 overexpression and iron supplementation (200 μM) for 48 h. (b) B-7 cells were grown for 48 h in the presence of FAC at different concentrations. (c) B-7 cells grown in doxycycline (Dox) at different concentrations for 96 h, and in 200 μM FAC for 48 h before analysis. Relaxation rates derived from the R_2 maps were expressed as mean $\pm$ SD for 3 experiments.

significantly increased the R_2 in B-7-cell-induced tumors but no-in parent-cell-induced tumors. These results indicate FTH1 overexpression can be detected by MRI and iron supplementation specifically increases the effect of FTH1 in MRI *in vivo*.

We also examined whether FTH1 overexpression could affect the tumor progression *in vivo*. The tumors overexpressing FTH1 with Fe supplementation grew in similar rate with parent-cell-induced tumors. However, as compared to the parent-cell-induced tumors, the tumors overexpressing FTH1 grew slower in the absence of Fe supplementation (Figure 6(d)).

3.5. In Vivo and Ex Vivo Validation of Luciferase and FTH1 Expression.

Subcutaneous B-7-cell-induced tumors and parent cell tumors were examined by hematoxylin-eosin (HE) staining, immunohistochemistry, and bioluminescence imaging (BLI). In the HE staining (Figures 7(a) and 7(b)), there was no detectable pathologic differences associated with FTH1 overexpression and iron supplementation. As expected, immunohistochemistry showed FTH1 overexpression was detectable in B-7-cell-induced tumors (Figure 7(d)) but not in parent cell tumors (Figure 7(c)). The luciferase activity in B-7-cell-induced tumors was increased up to 10^6 photons/sec while that in parent cell
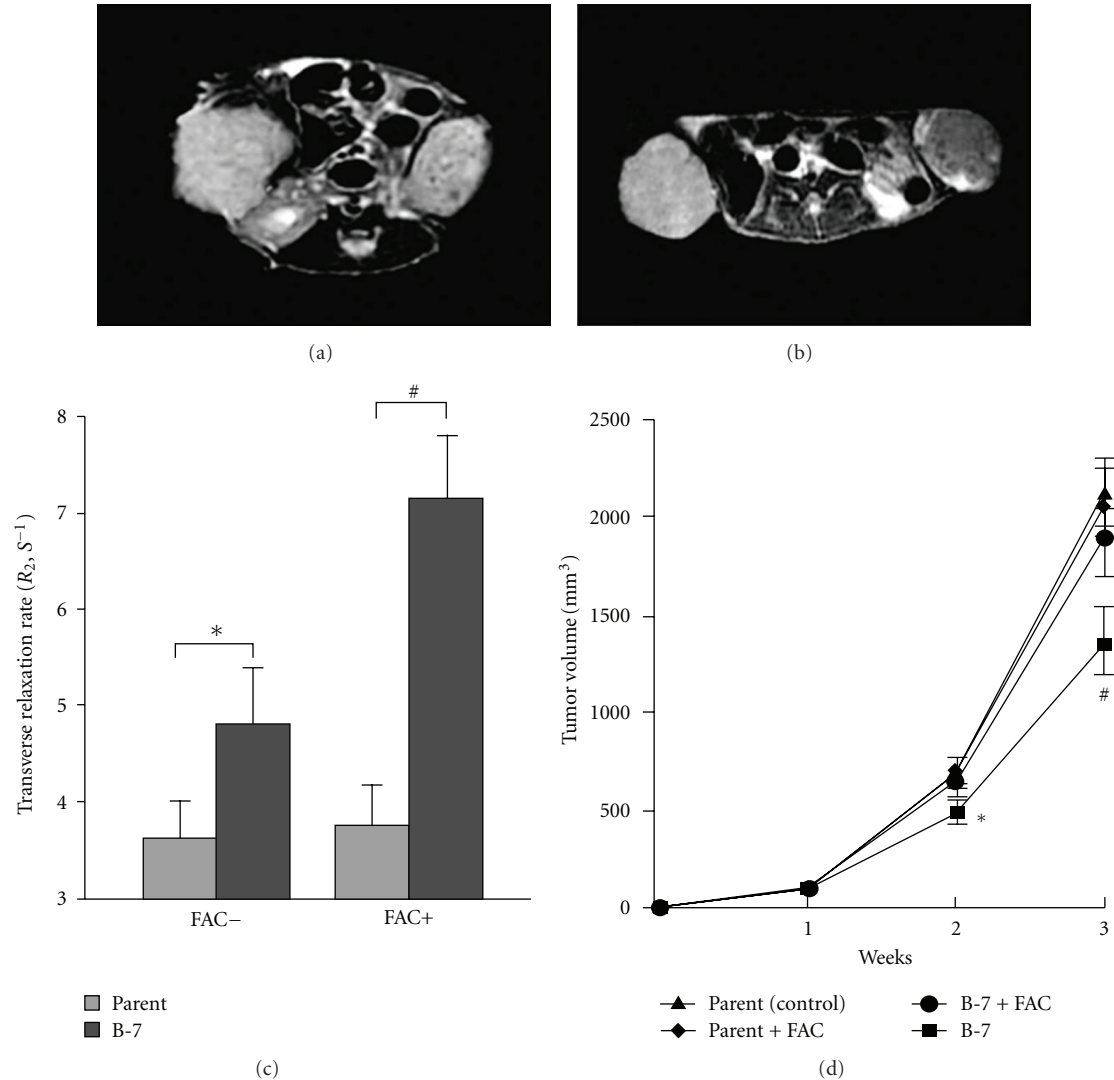
(a)

(b)

(c)

(d)

FIGURE 6: MRI of tumors over-expressing FTH1 *in vivo*. Representative T_2-wighted images of mice with inoculation of B-7 cells (right) and parent cells (left) were acquired at 21 days postinoculation without (a) or with (b) FAC supplementation in the drinking water. (c) R_2 at the tumor region. (d) Effects of FTH1 overexpression on the tumor growth. B-7 cells and parent cells were inoculated into the hind flank of nude mice, and tumor volumes were measured from MR images at the indicated time points. Data were expressed as mean $\pm$ SD for 6 experiments. ($^*P < 0.05$ and $^\#P < 0.01$.)

tumors remained unchanged (Figure 7(e)). To evaluate the impact of FTH1 overexpression on iron uptake, iron content of both parent cell and B-7-cell-induced tumors were quantified using ICP-MS (Figure 7(f)). Results indicated that the iron content was higher in B-7 cell induced tumors than in parent cell tumors, and FAC supplementation promoted the iron uptake in B-7-cell-induced tumors, but not in parent cell tumors.

4. Discussion

In the present study, our results demonstrated that MRI contrast due to FTH1 overexpression could be effectively detected and enhanced by iron supplementation in NPC S18

cells and xenografted tumors. These results were supported by *in vitro* and *in vivo* findings that FTH1 overexpression significantly increased the transverse relaxivities (R_2), which were enhanced by iron supplementation. Additionally, FTH1 overexpression led to some adverse effects on the proliferation and migration of S18 cells and the growth of xenografted tumors, and these effects were eliminated by iron supplementation.

In previous studies, findings showed FTH1 overexpression could increase the R_2 in C6 glioma cells [9], and stem cells [16, 17], and iron supplementation could affect the MRI contrast [29, 30]. Through overexpression of FTH1 in liver of transgenic mice (liver-hfer mice), Ziv et al. showed that overexpression of FTH1 increased iron absorption and elevated R_2 values compared to wildtype, and iron-enriched
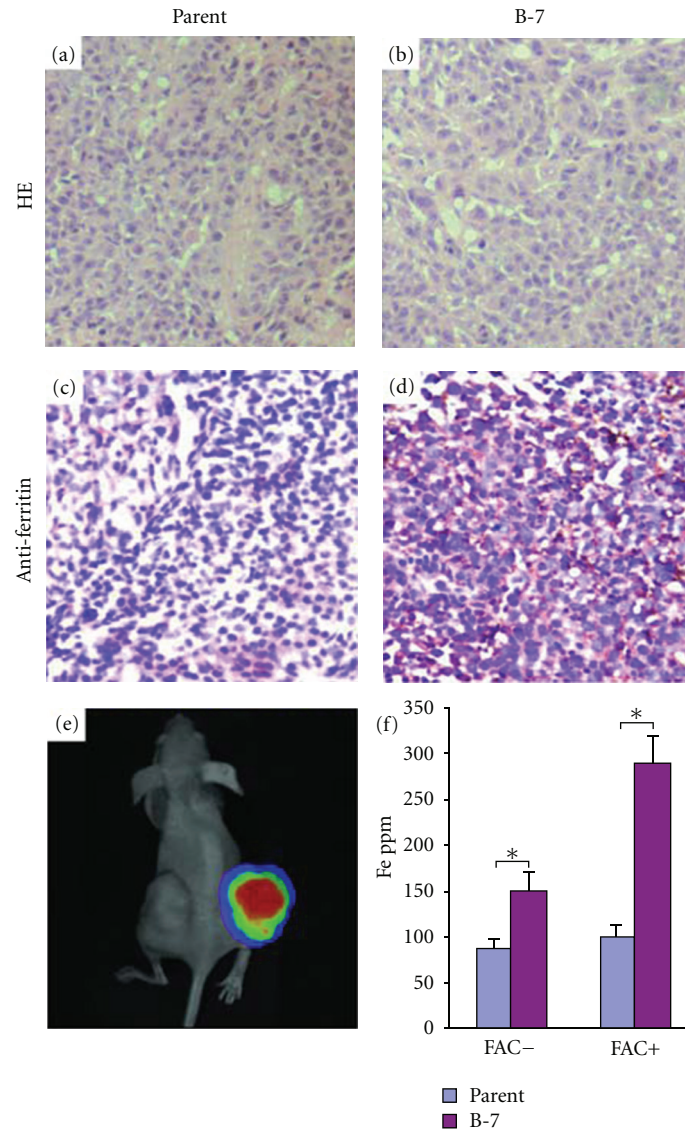
FIGURE 7: Parent cells (a and c) and B-7 cells (b and d) were inoculated into the hind flank of nude mice (left, parent cells; right, B-7 cells) with (FAC+) or without (FAC−) FAC supplementation in the drinking water. The tumors were collected for histological examination at the end of 3 weeks. (a and b) HE staining showed overexpression of FTH1 did not cause obvious pathological changes. (c and d) Immunohistochemistry demonstrated overexpression of FTH1 was easily detected in B-7-cell-induced tumors but not in parent-cell-induced tumors. (e) Luciferase activity detected by using bioluminescence imaging technology $in\ vivo$. Luciferase activity in B-7 cell induced tumors was increased up to 10^6 photons/sec, but that was not significantly changed in the parent-cell-induced tumors as compared to the background activity (<300 photons/sec). Representative image from mice in the presence of FAC. (f) ICP-MS analysis of Fe content measured in parts per million (ppm) dry weight of parent cells or B-7 cell induced tumors. Data were expressed as mean ± SD from 6 experiments. ($*P < 0.05$).

diet led to a significant elevation in R_2 values for both wildtype and liver-hfer mice, but no significant difference between wildtype and liver-hfer mice. It maybe that the hepatocyte itself was rich in iron [11], and the elevation in R_2 was not easily or significantly detected. Wang et al. showed that in xenografts derived from implanted C6 glioma cells, overexpression of FTH1 induced a minimal contrast in T_2-weighted MRI images. Also in C6 glioma cells labeled with SPIO (superparamagnetic iron oxide), overexpression of FTH1 significantly increased MRI contrast [30]. In the present study, our results showed the FTH1 overexpression

in NPC S18 cells could significantly increase the R_2 and iron supplementation could enhance the efficiency of FTH1. The signals from T_2 weight MR images acquired at 3.0 T were attenuated at the area of NPC xenografted tumors.

In our study, moderate overexpression of FTH1 in NPC S18 cells in the presence of 0.1 ng/mL doxycycline did not affect the cell growth with or without iron supplementation. The maximum of FTH1 overexpression in the absence of doxycycline reduced cell growth without iron supplementation but not in the presence of iron supplementation. These results were in accordance with the study of Cozzi et al. [22],

in which overexpression of FTH1 in Hela cells significantly reduced the cell growth, and this increase was reversed in the presence of iron supplementation. Additionally, Liu et al. [16] found that the growth of C6 glioma cells was reduced significantly when the FTH1 expression was dramatically increased. Hempstead et al. revealed the overexpression of mitochondrial ferritin dramatically reduced the growth of implanted tumors in nude mice [31]. In the present study, in other clones selected, clones with relatively high FTH1 level had not reduced cell growth with or without iron supplementation. This implies that remarkably high expression of FTH1 can decrease cell growth in certain types of cells.

Additionally, our results indicated significantly high expression of FTH1 reduced the migration of tumor cells in the absence of iron supplementation. A moderate overexpression of FTH1 had no effect on the migration of tumor cells regardless of the iron supplementation. These results implied that FTH1 overexpression could partially impair the biological behaviors of NPC S18 cells.

In previous studies, the findings on the effect of FTH1 on cells were inconsistent. One study revealed FTH1 increases the resistance to oxidative damage [22], but another showed overexpression of FTH1 results in iron accumulation and subsequent increase of reactive oxygen species [32]. Some reports showed FTH1 overexpression has degenerative effect on neurons [33] and metabolism in the brain (by MRS) [34], but others revealed FTH1 overexpression has no effects on the neurological system [34] and the liver [35]. In the present study, FTH1 overexpression did not increase reactive oxygen species (indirectly indicated by G6PD release) and apoptosis. Thus, the effect of ferritin may depend on cell types, degree of ferritin expression, and iron availability.

Overexpression of FTH1 causes transiently low level of intracellular free iron and thus leads to physiological compensation to augment iron uptake. Excessive intracellular iron can be sequestered within the over-expressed FTH1 pool. Our results showed in the presence of iron supplementation ($100 \sim 200 \mu$M FAC *in vitro*; 2 g/L in drinking water), overexpression of FTH1 could increase R_2 *in vitro* and *in vivo*. Thus, we speculate that when the FTH1 is highly over-expressed, more iron is needed to further enhance the sensitivity of MRI. Additionally, the phenomenon that iron supplementation can reverse the iron-deficient phenotype caused by FTH1 overexpression reminders us that, during the application of FTH1 as an MRI reporter, Fe at appropriate dose should be regularly administered during operation.

5. Conclusion

Our findings not only further support the effectiveness of FTH1 as an MRI reporter but also provide convincing evidence on its safety in clinical application. The present study elucidates that FTH1 can act effectively and safely as an MRI reporter with additional iron supplementation in monitoring NPC *in vitro* and *in vivo*. Therefore, FTH1 can be considered as promising MRI reporter in the NPC tracking.

Conflict of Interests

The authors declare that they have no competing interests.

Authors' Contributions

Y. Feng carried out the molecular genetic studies, participated in the sequence alignment, and drafted the manuscript. Q. Liu participated in the sequence alignment. J. Zhu carried out the cell culture. F. Xie participated in the design of the study and performed the statistical analysis. L. Li conceived of the study, participated in its design and coordination, and helped to draft the manuscript. All authors read and approved the final manuscript. Y. Feng and Q. Liu contributed equally to this work.

Acknowledgment

References

[1] M. Comoretto, L. Balestreri, E. Borsatti, M. Cimitan, G. Franchin, and M. Lise, "Detection and restaging of residual and/or recurrent nasopharyngeal carcinoma after chemotherapy and radiation therapy: comparison of MR imaging and FDG PET/CT," *Radiology*, vol. 249, no. 1, pp. 203–211, 2008.

[2] L. Z. Liu, G. Y. Zhang, C. M. Xie, X. W. Liu, C. Y. Cui, and L. Li, "Magnetic resonance imaging of retropharyngeal lymph node metastasis in nasopharyngeal carcinoma: patterns of spread," *International Journal of Radiation Oncology Biology Physics*, vol. 66, no. 3, pp. 721–730, 2006.

[3] S. H. Ng, J. T. Chang, S. C. Chan et al., "Nodal metastases of nasopharyngeal carcinoma: patterns of disease on MRI and FDG PET," *European Journal of Nuclear Medicine and Molecular Imaging*, vol. 31, no. 8, pp. 1073–1080, 2004.

[4] G. Y. Zhang, L. Z. Liu, W. H. Wei, Y. M. Deng, Y. Z. Li, and X. W. Liu, "Radiologic criteria of retropharyngeal lymph node metastasis in nasopharyngeal carcinoma treated with radiation therapy," *Radiology*, vol. 255, no. 2, pp. 605–612, 2010.

[5] M. Lewin, N. Carlesso, C. H. Tung et al., "Tat peptide-derivatized magnetic nanoparticles allow in vivo tracking and recovery of progenitor cells," *Nature Biotechnology*, vol. 18, no. 4, pp. 410–414, 2000.

[6] A. Y. Louie, M. M. Hüber, E. T. Ahrens et al., "In vivo visualization of gene expression using magnetic resonance imaging," *Nature Biotechnology*, vol. 18, no. 3, pp. 321–325, 2000.

[7] F. Podo, "Tumour phospholipid metabolism," *NMR in Biomedicine*, vol. 12, no. 7, pp. 413–439, 1999.

[8] P. M. Winter, S. D. Caruthers, A. Kassner et al., "Molecular imaging of angiogenesis in nascent Vx-2 rabbit tumors using a novel $\alpha_v \beta_3$-targeted nanoparticle and 1.5 tesla magnetic resonance imaging," *Cancer Research*, vol. 63, no. 18, pp. 5838–5843, 2003.

[9] B. Cohen, H. Dafni, G. Meir, A. Harmelin, and M. Neeman, "Ferritin as an endogenous MRI reporter for noninvasive imaging of gene expression in C6 glioma tumors," *Neoplasia*, vol. 7, no. 2, pp. 109–117, 2005.

[10] G. Genove, U. DeMarco, H. Xu, W. F. Goins, and E. T. Ahrens, "A new transgene reporter for in vivo magnetic resonance imaging," *Nature Medicine*, vol. 11, no. 4, pp. 450–454, 2005.

[11] B. Cohen, K. Ziv, V. Plaks et al., "MRI detection of transcriptional regulation of gene expression in transgenic mice," *Nature Medicine*, vol. 13, no. 4, pp. 498–503, 2007.

[12] A. Treffry, Z. Zhao, M. A. Quail, J. R. Guest, and P. M. Harrison, "Dinuclear center of ferritin: studies of iron binding and oxidation show differences in the two iron sites," *Biochemistry*, vol. 36, no. 2, pp. 432–441, 1997.

[13] M. De, P. S. Ghosh, and V. M. Rotello, "Applications of nanoparticles in biology," *Advanced Materials*, vol. 20, no. 22, pp. 4225–4241, 2008.

[14] A. K. Gupta, R. R. Naregalkar, V. D. Vaidya, and M. Gupta, "Recent advances on surface engineering of magnetic iron oxide nanoparticles and their biomedical applications," *Nanomedicine*, vol. 2, no. 1, pp. 23–39, 2007.

[15] B. Iordanova, C. S. Robison, and E. T. Ahrens, "Design and characterization of a chimeric ferritin with enhanced iron loading and transverse NMR relaxation rate," *Journal of Biological Inorganic Chemistry*, vol. 15, no. 6, pp. 957–965, 2010.

[16] J. Liu, E. C. H. Cheng, R. C. Long et al., "Noninvasive monitoring of embryonic stem cells in vivo with MRI transgene reporter," *Tissue Engineering C*, vol. 15, no. 4, pp. 739–747, 2009.

[17] A. V. Naumova, H. Reinecke, V. Yarnykh, J. Deem, C. Yuan, and C. E. Murry, "Ferritin overexpression for noninvasive magnetic resonance imaging-based tracking of stem cells transplanted into the heart," *Molecular Imaging*, vol. 9, no. 4, pp. 201–210, 2010.

[18] M. Ueda, T. Kudo, Y. Kuge et al., "Rapid detection of hypoxia-inducible factor-1-active tumours: pretargeted imaging with a protein degrading in a mechanism similar to hypoxia-inducible factor-1alpha," *European Journal of Nuclear Medicine and Molecular Imaging*, vol. 37, no. 8, pp. 1566–1574, 2010.

[19] M. Campan, V. Lionetti, G. D. Aquaro et al., "Ferritin as a reporter gene for in vivo tracking of stem cells by 1.5-T cardiac MRI in a rat model of myocardial infarction," *American Journal of Physiology*, vol. 300, no. 6, pp. 2238–2250, 2011.

[20] H. S. Kim, H. R. Cho, S. H. Choi, J. S. Woo, and W. K. Moon, "In vivo imaging of tumor transduced with bimodal lentiviral vector encoding human ferritin and green fluorescent protein on a 1.5T clinical magnetic resonance scanner," *Cancer Research*, vol. 70, no. 18, pp. 7315–7324, 2010.

[21] G. Velde, J. R. Vande, J. Rangarajan et al., "Evaluation of the specificity and sensitivity of ferritin as an MRI reporter gene in the mouse brain using lentiviral and adeno-associated viral vectors," *Gene Therapy*, vol. 18, pp. 594–605, 2011.

[22] A. Cozzi, B. Corsi, S. Levi, P. Santambrogio, A. Albertini, and P. Arosio, "Overexpression of wild type and mutated human ferritin H-chain in HeLa cells: in vivo role of ferritin ferroxidase activity," *Journal of Biological Chemistry*, vol. 275, no. 33, pp. 25122–25129, 2000.

[23] W. I. Wei and J. S. T. Sham, "Nasopharyngeal carcinoma," *The Lancet*, vol. 365, no. 9476, pp. 2041–2054, 2005.

[24] C. N. Qian, B. Berghuis, G. Tsarfaty et al., "Preparing the "soil": the primary tumor induces vasculature reorganization in the sentinel lymph node before the arrival of metastatic cancer cells," *Cancer Research*, vol. 66, no. 21, pp. 10365–10376, 2006.

[25] L. Flatz, A. N. Hegazy, A. Bergthaler et al., "Development of replication-defective lymphocytic choriomeningitis virus vectors for the induction of potent CD8+ T cell immunity," *Nature Medicine*, vol. 16, no. 3, pp. 339–345, 2010.

[26] S. Urlinger, U. Baron, M. Thellmann, M. T. Hasan, H. Bujard, and W. Hillen, "Exploring the sequence space for tetracycline-dependent transcriptional activators: novel mutations yield expanded range and sensitivity," *Proceedings of the National Academy of Sciences of the United States of America*, vol. 97, no. 14, pp. 7963–7968, 2000.

[27] M. W. Hentze, M. U. Muckenthaler, and N. C. Andrews, "Balancing acts: molecular control of mammalian iron metabolism," *Cell*, vol. 117, no. 3, pp. 285–297, 2004.

[28] D. Kivelitz, H. B. Gehl, A. Heuck et al., "Ferric ammonium citrate as a positive bowel contrast agent for MR imaging of the upper abdomen. Safety and diagnostic efficacy," *Acta Radiologica*, vol. 40, no. 4, pp. 429–435, 1999.

[29] K. Ziv, G. Meir, A. Harmelin, E. Shimoni, E. Klein, and M. Neeman, "Ferritin as a reporter gene for MRI: chronic liver over expression of H-ferritin during dietary iron supplementation and aging," *NMR in Biomedicine*, vol. 23, no. 5, pp. 523–531, 2010.

[30] J. Wang, J. Xie, X. Zhou et al., "Ferritin enhances SPIO tracking of C6 rat glioma cells by MRI," *Molecular Imaging and Biology*, vol. 13, no. 1, pp. 87–93, 2011.

[31] P. D. Hempstead, S. J. Yewdall, A. R. Fernie et al., "Comparison of the three-dimensional structures of recombinant human H and horse L ferritins at high resolution," *Journal of Molecular Biology*, vol. 268, no. 2, pp. 424–448, 1997.

[32] A. E. Deans, Y. Z. Wadghiri, L. M. Bernas, X. Yu, B. K. Rutt, and D. H. Turnbull, "Cellular MRI contrast via coexpression of transferrin receptor and ferritin," *Magnetic Resonance in Medicine*, vol. 56, no. 1, pp. 51–59, 2006.

[33] D. Kaur, S. Rajagopalan, S. Chinta et al., "Chronic ferritin expression within murine dopaminergic midbrain neurons results in a progressive age-related neurodegeneration," *Brain Research*, vol. 1140, no. 1, pp. 188–194, 2007.

[34] S. Hasegawa, S. Saito, J. Takanashi et al., "Evaluation of ferritin-overexpressing brain in newly developed transgenic mice," *Magnetic Resonance Imaging*, vol. 29, no. 2, pp. 179–184, 2011.

[35] K. Ziv, G. Meir, A. Harmelin, E. Shimoni, E. Klein, and M. Neeman, "Ferritin as a reporter gene for MRI: chronic liver over expression of h-ferritin during dietary iron supplementation and aging," *NMR in Biomedicine*, vol. 23, no. 5, pp. 523–531, 2010.